Synthesis, Characterization, and Activity in the Epoxidation of Cyclohexene with Aqueous H_2O_2 of Catalysts Prepared by Reaction of TiF_4 with Silica

E. Jorda,* A. Tuel,*,[1] R. Teissier,† and J. Kervennal†

*Institut de Recherches sur la Catalyse, C.N.R.S., 2, avenue A. Einstein 69626, Villeurbanne Cedex, France; and †Elf Atochem, CRRA, rue H. Moissan, BP 30, 69310, Pierre Bénite Cedex, France

Ti-supported silica materials have been prepared by reaction between TiF_4 and silica in the liquid phase. Samples prepared in an organic solvent contain titanium and fluorine, but the fluorine can easily be removed upon treatment with ammonia. Directly defluorinated samples can be synthesized in aqueous NH_4OH solutions and are similar to those obtained in an organic medium after basic treatment. For low Ti contents (typically <2 wt%), titanium is highly dispersed on the silica surface in the form of isolated tetrahedrally coordinated Ti(IV) species or TiO_2 domains, whose size does not exceed a few nanometers. Most of these TiO_2 particles can be removed upon washing with concentrated acid. These materials possess a Lewis acidity, due to both isolated Ti centers and TiO_2 nanoparticles, and catalyze the epoxidation of cyclohexene with concentrated aqueous H_2O_2 solutions. The reaction mainly proceeds by a radical mechanism, leading to the formation of allylic oxidation products like cyclohexenyl hydroperoxide. This intermediate reacts further with cyclohexene to cyclohexene oxide and cyclohexenol in similar amounts. Nevertheless, part of the H_2O_2 initially introduced is also used for the direct nonradical epoxidation of cyclohexene to cyclohexene oxide. Both direct epoxidation and bimolecular reaction between cyclohexenyl hydroperoxide and cyclohexene are inhibited in the presence of water. However, water does not influence the formation of cyclohexenyl hydroperoxide that occurs in the absence, as well as in the presence, of water. On the contrary, dropwise addition of H_2O_2 favors the nonradical epoxidation of cyclohexene to cyclohexene oxide in relatively high yields. Maximum epoxide selectivities are obtained over catalysts containing less than 2 wt% Ti, whilst higher loading leads to the formation of cyclohexanediol, formed on the Brönsted sites of the materials.   © 1998 Academic Press

Key Words: titanium; TiF_4; epoxidation; hydrogen peroxide; cyclohexene.

I. INTRODUCTION

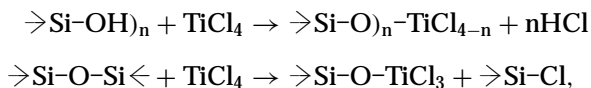There has been an increasing interest over the last years for the development of heterogeneous catalysts for oxidation reactions in the liquid phase with aqueous H_2O_2 or organic hydroperoxides. This was partially achieved by using transition metal-containing zeolites or aluminophosphates which proved to be remarkable catalysts for the oxidation of a large family of small organic molecules with both H_2O_2 and tert-butyl hydroperoxide (TBHP) (1). However, as far as microporous molecular sieves are concerned, reactions are limited to substrates capable of entering the zeolite pores, i.e. with a kinetic diameter smaller than ca 7 Å. Moreover, these materials are often expensive and relatively difficult to synthesize, as their preparation requires specific conditions to prevent the formation of metal oxide species during the crystallization process. The activity of these catalysts in oxidation reactions has been attributed to the presence of isolated metal sites in a silica or aluminophosphate framework.

Because of these limitations due to the presence of micropores, many attempts have been made to replace these zeolite-based catalysts by systems containing highly dispersed transition metal cations on various organic or inorganic supports with high surface areas (2). There has been an important breakthrough with the recent discovery of metal-containing mesoporous silicas that were shown to possess interesting properties in the oxidation of bulky substrates (3–5). It was also reported that SiO_2–TiO_2 mixed oxides could catalyze the epoxidation of olefins with TBHP or other alkyl hydroperoxides (6–11). The physicochemical properties of these materials depend on a lot of factors, but synthesis methods have been developed recently in which the pore distribution and the titanium dispersion are greatly improved (12). As for zeolitic materials, high activities are observed when the mixed oxides possess highly dispersed titanium species, high surface areas, and a meso or microporous structure.

Concerning transition metal-supported materials, the system Ti/SiO_2 has shown very attractive properties for epoxidation reactions with organic hydroperoxides. This catalyst was originally developed by Shell in the early 1970s

by reacting silica with TiCl$_4$ or organic titanium compounds, followed by a calcination (13, 14). Unfortunately, such a method does not always lead to highly dispersed Ti species on silica and TiO$_2$ particles are often formed, particularly for high Ti loadings. Therefore, new approaches have been used recently to increase the dispersion of Ti species on the silica surface. The most commonly used consist in grafting titanium on the surface by the reaction of TiCl$_4$ or Ti-alkoxides with hydroxyl groups or siloxane bridges,

$$\rangle Si{-}OH)_n + TiCl_4 \rightarrow \rangle Si{-}O)_n{-}TiCl_{4-n} + nHCl$$

$$\rangle Si{-}O{-}Si\langle + TiCl_4 \rightarrow \rangle Si{-}O{-}TiCl_3 + \rangle Si{-}Cl,$$

where the value of n strongly depends on the reaction conditions, as well as on the pore structure and thermal pretreatment of the silica. There is considerable literature on the characterization of species formed by the reaction of TiCl$_4$ with silica (15–20). More recently, new titanium–silica catalysts for epoxidation reactions with TBHP have been prepared by treating a silica gel with titanium isopropoxide in toluene (21, 22). Oldroyd *et al.* (23) also prepared Ti grafted onto the inner surface of mesoporous silica MCM-41 and showed that the material was much more active than Ti-MCM-41 prepared by direct synthesis in the epoxidation of cyclohexene with 2-methyl-1-phenyl-2-propyl hydroperoxide (MPPH).

In fact, these systems are usually not catalytically active in oxidation reactions when aqueous H$_2$O$_2$ is used as the oxidant (24–26). The reason is that the environment of catalytic sites is very different from that existing in zeolites like TS-1. Indeed, the hydrophilic character of the silica surface makes that Ti sites are surrounded by water molecules, which considerably decreases their efficiency in these reactions. The influence of water on catalytic sites is not fully understood but experiments performed under azeotropic distillation or over hydrophobic supports have shown that the activity could be significantly increased (26).

We have recently reported the synthesis of new TiF$_4$/SiO$_2$ materials, active in epoxidation reactions with aqueous hydrogen peroxide solutions (27). In the present paper, we report on the synthesis of these solids and their detailed characterization by means of spectroscopic techniques. Adsorption of probe molecules was also monitored by infra red spectroscopy in order to obtain information about the nature of the modified silica surface. The state of Ti species as a function of titanium loading and a possible mechanism for the reaction of TiF$_4$ with silica are discussed.

These materials have been used as catalysts in the epoxidation of cyclohexene with aqueous hydrogen peroxide solutions. The influence of the preparation route, of postsynthesis treatments, and of the Ti content on the performance of the solids are discussed. A reaction mechanism, involving both radical and nonradical pathways is proposed.

II. EXPERIMENTAL

1. Synthesis

Catalysts were prepared in the liquid phase by reacting TiF$_4$ (Aldrich) with silica following two different methods.

Method 1. We have previously reported that these catalysts could be prepared using a two-step route, which consists in reacting TiF$_4$ with silica in an organic solvent followed by a defluorination of the sample with an inorganic base (27). In a typical preparation, 1.94 g of TiF$_4$ is introduced into 500 ml of solvent and the solution is stirred at 60°C for about 30 min. Fifty grams of silica (precipitated silica FK 310 from Degussa, 650 m^2/g) are then rapidly added and stirring is maintained at 60°C for about 2 h. After this period, the solid is recovered by filtration and dried under vacuum at 120°C for 12 h. Different solvents have been tested, namely diglyme (2-methoxyethyl ether), acetone, and water. Calcination of the samples was performed at 500°C in air for 3 h.

As will be discussed later, at this stage of the synthesis, samples contain relatively large amounts of fluorine. Thus, they can be defluorinated by washing with alkali solutions. Typically, 1 g of solid is dispersed in 20 ml of distilled water. A molar solution of NaOH or NH$_4$OH is then added dropwise under vigorous stirring until the pH of the solution is about 8. The solid is then recovered by filtration, washed several times with distilled water, and dried at 120°C under vacuum. This treatment removes almost entirely fluorine from the samples but it does not affect the Ti content.

Method 2. Due to the remarkable stability of TiF$_4$ in basic aqueous solutions, we have developed a second method of preparation in which the grafting of Ti species and defluorination of the samples are performed in one step (28). In contrast to Method 1, all the preparation is carried out in water at room temperature. Typically, 10 g of silica FK 310 (Degussa) is dispersed in 100 ml of distilled water under stirring. The pH of the solution is then increased to about 10 by the addition of ammonia (28 wt% in water). After 5 min, 0.4 g of TiF$_4$ is added and the pH is adjusted to 8 by careful addition of ammonia. The suspension is stirred for 30 min and the solid is recovered by filtration and dried at 120°C.

For both methods, several samples have been prepared by varying the amount of TiF$_4$ introduced in the reaction mixture.

2. Characterization

Infra red spectra were collected in the 400–4000 cm^{-1} range on a Bruker IFS 48 FTIR spectrometer. For each spectrum, 100 scans were accumulated. Framework spectra were obtained using the KBr method (1 wt% of the sample in KBr). For infra red studies of probe molecules,

self-supported wafers of typically 15 mg were used. These wafers were placed in a pyrex cell equipped with KBr windows. They were first calcined at 500°C under O_2 for 6 h and evacuated for 1 h under vacuum (10^{-5} Torr) prior to the admission of pyridine. A known amount of pyridine was then introduced on the wafer at room temperature. After 5 min, pyridine was desorbed under vacuum for 15 min at room temperature. The next desorption was performed at 50°C for 1 h. The IR spectrum thus obtained was used to calculate the amount of acid sites on the sample by measuring the areas of pyridine adsorption peaks. UV-Vis spectra were obtained with a Perkin Elmer λ9 spectrometer.

XPS spectra have been recorded on a Escalab 200 R (Fisons Instruments) spectrometer using the MgKα radiation. Samples were placed on an indium grid and analyzed under a pressure of 10^{-9} Torr, with a precision of about 0.2–0.3 eV in the line position.

SEM pictures were obtained on a Hitachi S 800 microscope. For TEM pictures, a Jeol JEM 2010 (200 kV) microscope equipped with an EDX probe was used.

The titanium content was determined by ICP after solubilization of the samples in HF : HCl solutions. For fluorine, samples were first mineralized with K_2CO_3 and Na_2CO_3 and the fluorine content was measured using a selective electrode.

3. Catalytic Tests

The epoxidation of cyclohexene was performed under ambient atmosphere in a round-bottomed flask equipped with a condenser and a magnetic stirrer. In a typical reaction, 1 g of catalyst was dispersed in a solution containing cyclohexene (25 ml) and diglyme (15 ml) and the temperature was increased to 90°C; 5 ml of diglyme containing 11 mmol H_2O_2 (70 wt% in water) were then introduced either in one lot or over 1 h. After complete addition of the oxidizing agent, the Ti : alkene : oxidant ratio was 0.3 : 250 : 11. Samples were taken at constant time intervals and analyzed by gas chromatography using a Carbowax (AT-wax) column (Alltech) attached to a FID detector. The amount of oxygen evolved during the reaction was measured using a calibrated column filled with water and connected to the condenser. In some experiments, anhydrous *tert*-butyl hydroperoxide (TBHP, 95 wt% in cyclohexane) has also been used as the oxidizing agent, instead of H_2O_2.

III. RESULTS AND DISCUSSION

1. Characterization of the Catalysts

1.1. Dispersion of titanium species. Method 1. The chemical composition of a material synthesized in diglyme following Method 1 of the Experimental section gives 1.35 wt% Ti and 2.32 wt% F. After calcination, these values are 1.55 wt% Ti and 2.4 wt% F and are very close to the expected values (1.5 wt% Ti and 2.37 wt% F). This indicates that all Ti and F species originally introduced in the reaction mixture are present on the silica surface in the as-synthesized and calcined forms of the solid. However, the percentages of Ti and F retained on the silica surface depend on the nature of the solvent in which the reaction is performed. Whilst excellent results are obtained in diglyme, about only 85% of Ti and 80% of F initially introduced are on the silica surface when the reaction is carried out in acetone. These values are even lower in water, where only 60% of titanium and 30% of fluorine are retained on silica. For this reason, most of the materials prepared following this method were synthesized in diglyme.

The UV-Vis spectrum of the dried sample showed an adsorption band with a maximum at ca 220–230 nm, and no signal above 310 nm characteristic of TiO_2-like species. The signal was very similar to that observed on SiO_2–TiO_2 mixed oxides, or Ti-containing mesoporous silicas, and has been attributed either to isolated tetrahedrally coordinated Ti species, along with some re-hydrated five- and six-coordinated species or to titania nanodomains (7, 29, 30). It is interesting to note that the spectrum was very different from that of TiF_4 in diglyme. Indeed, the latter was composed of a sharp absorption at 272 nm and characterized isolated octahedrally coordinated species (27). The UV-Vis spectrum of the dried sample was not significantly modified upon calcination in air at 500°C. More interesting was the absence of signal around 330 nm, which indicated that TiO_2 had not been formed upon calcination at high temperature.

The framework IR spectra of both dried and calcined samples show the typical absorption bands of amorphous silica at ca 1210, 1070, 960, 800, and 450 cm^{-1}. In addition, a weak absorption is observed for both samples at 720 cm^{-1} that is absent from the spectrum of silica FK 310 before treatment (Fig. 1). Such a band has been previously observed on chlorinated silicas and was attributed to a ν_{Si-Cl} vibration mode (31). When the silica support FK 310 is treated with a dilute solution of HF, the IR band at 720 cm^{-1} is also observed, and we can unambiguously attribute it to a vibration mode of Si–F bonds. This suggests that, even though all Ti and F are present on the silica surface, they are not present in the form of TiF_4, which is probably partially dissociated in the reaction medium.

Additional information about surface species has been obtained from XPS. The F1s line of the dried material shows a major peak at 687.1 eV with a shoulder at 684.6 eV (Fig. 2). For comparison, a single line is observed at 685.3 eV on TiF_4 and at 686.9 eV on fluorinated silica. Deconvolution of the F1s line of the dried solid gives approximately 75% of species with a binding energy of 687.1 eV and 25% of species with a binding energy of 684.6 eV. The binding energies of hexafluorosilicate and hexafluorotitanate compounds clearly show an increase in energy from
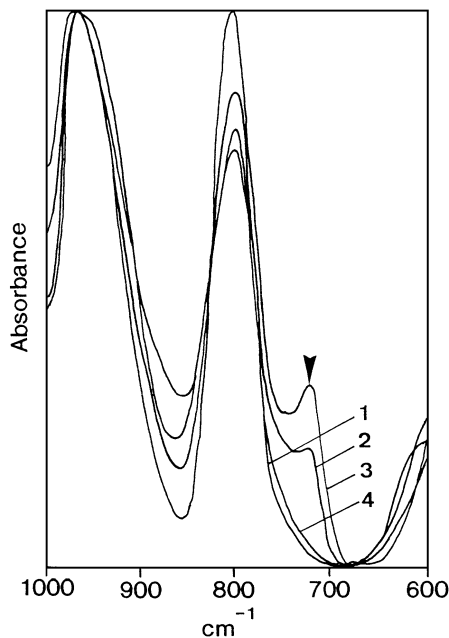
FIG. 1. Framework IR spectra of silica FK 310 (1), Ti/SiO$_2$ as-synthesized (2), FK 310 treated with HF (3), and Ti/SiO$_2$ calcined and washed with ammonia (4).

titanium to silicon (Table 1). The values for hexafluorosilicates and hexafluorotitanates are close to the values of 687.1 and 684.6 eV observed on the dried material. Therefore, we can propose that, on the dried solid, about 75% of fluorine is in the form of Si–F bonds with a binding energy of 687.1 eV, whereas 25% is still bonded to titanium with a binding energy of 684.6 eV. After calcination at 500°C, the shoulder at 684.6 eV disappears and only one line is observed at 687.3 eV, suggesting that titanium is totally defluorinated upon calcination (Fig. 2).
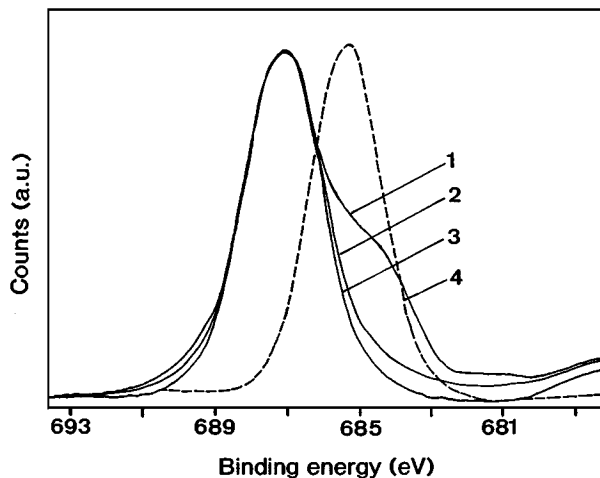

FIG. 2. F1s XPS lines of Ti/SiO$_2$ as-synthesized (1) and calcined (2); FK 310 treated with HF (3), and TiF$_4$ (4).

TABLE 1

**F1s XPS Binding Energies of Hexafluorosilicate and Hexafluorotitanate Compounds**

	K$_2$SiF$_6$	K$_2$TiF$_6$	Na$_2$SiF$_6$	Na$_2$TiF$_6$
F1s (eV)	686.6	685	686.2	685.3

The Ti2p3/2 binding energy of dried and calcined materials was between those of TiF$_4$ (460.8 eV) and TiO$_2$ (458.5 eV), indicating that oxygen atoms were present in the first coordination sphere of titanium. The XPS line was quite broad, which may indicate that Ti could be present on the silica surface in various environments. It was interesting to note that the binding energies were quite close to that obtained on Ti-silicalites, where titanium is tetrahedrally coordinated (32).
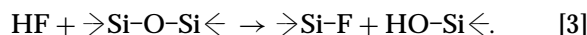
Washing the dried material with a 1 N solution of ammonia results in the removal of almost 95% of the fluorine from the silica surface. The chemical analysis of the defluorinated sample gives 1.32 wt% Ti and less than 0.1 wt% F, which shows that, in contrast to fluorine, titanium is not removed during the treatment. As expected, the band at 720 cm^{-1} present in the IR spectra of dried and calcined samples is not observed anymore (Fig. 1). The dispersion of titanium on the silica surface was not affected by the basic treatment as evidenced by UV-Vis spectroscopy.

From these observations, it is now possible to propose a reaction scheme between silica and TiF$_4$ in an organic solvent.

First, TiF$_4$ reacts with silanol groups of the silica surface and is partially defluorinated:

$$\mathord{>}\text{Si–OH} + \text{TiF}_4 \xrightarrow{\text{diglyme}} \mathord{>}\text{Si–O})_{3-n}\text{–Ti(OH)}_n\text{F} + 3\text{HF}. \tag{1}$$
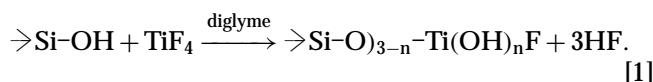
The percentages of Ti and F fixed on the silica surface depend on the silanol population. When a fumed silica A 200 (Degussa) is used instead of FK 310, only about 65% of titanium is retained on the surface. Even though it is very difficult to determine the value of n from spectroscopic data, XPS has clearly shown that the average number of Ti–F bonds is close to one in dried samples. HF reacts then with the silica surface to form Si–F bonds:

$$\text{HF} + \mathord{>}\text{Si–O–H} \rightarrow \mathord{>}\text{Si–F} + \text{H}_2\text{O} \tag{2}$$

$$\text{HF} + \mathord{>}\text{Si–O–Si}\mathord{<} \rightarrow \mathord{>}\text{Si–F} + \text{HO–Si}\mathord{<}. \tag{3}$$

Upon calcination in air at 500°C, the last Ti–F bond is cleaved and hydrofluoric acid reacts with the silica surface,

$$\mathord{>}\text{Si–O})_{3-n}\text{–Ti(OH)}_n\text{F} \rightarrow$$

$$\mathord{>}\text{Si–O})_{4-m}\text{–Ti(OH)}_m + \text{HF} \quad (m < 4) \tag{4}$$
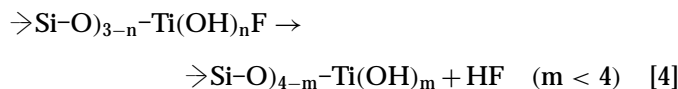
and the released HF reacts with the silica surface again as in Eqs. [2] and [3].

TABLE 2

Ti Contents (wt%) in Samples Washed with Various Solvents

	Solvent				
Sample[a]	No treatment	Water[b]	H_2O_2[c]	HCl (6 M)	H_2SO_4 (6 M)
Ti/SiO$_2$ (A.S.)	1.25	1.3	0.1	Traces	Traces
Ti/SiO$_2$ (C)	1.33	1.35	0.90	0.87	0.64
Ti/SiO$_2$ (C + D)	1.13	1.18	0.73	0.46	0.34

[a] Samples are as-synthesized (A.S.), calcined (C), or calcined and defluorinated with NH$_4$OH (C + D).
[b] Hot water at 80°C.
[c] Aqueous H$_2$O$_2$ solution (30 wt% in water).

TABLE 3

Ti and F Contents (wt%) in Samples Prepared in Water at Different pH Values and Subsequently Washed with HNO$_3$ (6M)

pH	1	2	4	6	8	10
F (wt%)	0.96	1.14	0.97	1.21	0.41	0.4
Ti (wt%)	0.61	0.79	0.85	1.11	1.33	1.35
Ti (wt%)[a]	Traces	0.3	0.33	0.35	0.48	0.57

[a] Samples washed with HNO$_3$ (6 M).

Calcination increases the number of oxygen atoms in the first coordination sphere around Ti, which probably reinforces its attachment to the silica surface. In order to estimate the nature and strength of bindings between Ti species and silica, samples have been washed with various solvents and subjected to characterization (Table 2). For each experiment, 10 g of catalyst were dispersed in the solvent under vigorous stirring. Stirring was maintained for 1 h and the solid was recovered by filtration, washed with distilled water, and dried at 120°C. Whilst hot water has no effect on both dried and calcined materials, the percentage of Ti removed by strong acidic solutions depends on whether the solids are calcined or not. For dried samples, only traces of titanium are still present after washing with 6 M HCl or 3 M H$_2$SO$_4$. On the other hand, approximately 65 and 48% of titanium are still present when calcined samples are washed with HCl and H$_2$SO$_4$, respectively. This is in agreement with the fact that the number of Si–O–Ti bridges is probably higher in calcined samples, which makes the extraction of Ti species more difficult. Indeed, tetrahedrally coordinated Ti atoms in TS-1 are very resistant to similar treatments since only about 7% of titanium is removed by 3 MH$_2$SO$_4$ solutions. For Ti/SiO$_2$ materials, we have observed that the totality of extractable titanium was removed upon the first washing and that further treatments had no effect on the Ti content.

The UV-Vis spectra of washed samples were significantly different from those of untreated samples. The maximum of absorption was blue-shifted to 215 nm and the intensity of the signal in the 250–300 nm region was lower. Basically, the spectra were identical to that of TS-1, which suggested that the nonextractable titanium was isolated and possessed a tetrahedral coordination. This supports the idea that Ti could be present on the silica surface in different environments, which was already stipulated from XPS spectra. On calcined samples, 40 to 50% of Ti species are easily extractable with strong acids whilst the remaining species are strongly bonded, in an environment similar to that of Ti in TS-1.

Method 2. Since TiF$_4$ is very stable in aqueous solutions even at relatively high pH values, we have explored the possibility of preparing materials in water (Method 2), which offers advantages with respect to organic solvents. In particular, a preparation in the presence of NH$_4$OH could provide directly defluorinated samples. A series of samples has been synthesized at different pH values by the addition of HCl or NH$_4$OH to a suspension of silica in water. Chemical analysis of the samples shows that the amount of Ti retained on the silica surface increases with the pH value and that almost all Ti is in the solid phase for pH > 8 (Table 3). In acidic solutions, fluorine is present in the samples. However, in contrast to titanium, the amount of fluorine fixed on silica is always close to 1 wt% and does not seem to depend on the pH value of the solution. As expected, samples prepared in basic solutions are highly defluorinated, with a F/Ti ratio of ca 0.7. UV-Vis spectra of the various samples show an intense absorption between 230 and 240 nm (Fig. 3). The intensity in the 270–350 nm region is lower for samples prepared in basic solutions than for samples prepared in the presence of HCl. The spectrum of the sample prepared at pH = 10 is very similar to that of a material prepared in diglyme and subsequently defluorinated. Different interpretations of UV-Vis spectra have been reported in the literature to explain the position and width of the
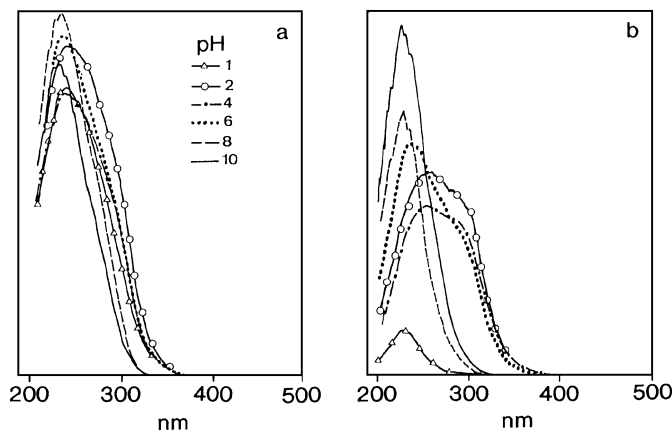

FIG. 3. UV/Vis spectra of Ti/SiO$_2$ catalysts prepared in water at different pH values. (a) as-synthesized materials; (b) solids calcined and washed with HNO$_3$ (6 M).
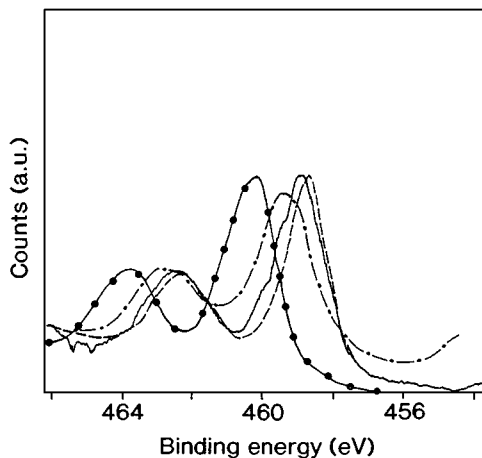
FIG. 4. Ti2p$_{3/2}$ XPS lines of TS-1 (–●–), TiO$_2$ (– – –), and Ti/SiO$_2$ prepared at pH = 10, as-synthesized (——), calcined and washed with HNO$_3$ (6 M) (–•–).

absorption band. It is usually accepted that a charge transfer band at 220 nm is characteristic of isolated, tetrahedrally coordinated Ti(IV) species in a silica matrix (30). Signals at higher wave numbers (240–280 nm) can be interpreted in terms of higher coordinations for Ti species (5 to 6) or by the presence of titania nanodomains in the materials.

A close examination of the Ti2p3/2 XPS line of the sample prepared at pH = 10 shows that this line is too broad to be assigned to a single environment of titanium on the surface (Fig. 4). A raw deconvolution gave two components, one at 458.1 eV with a binding energy close to that of TiO$_2$ and another one at 459.4 eV, in a ratio of about 1 : 2. The first line could be assigned to TiO$_2$ nanodomains on the silica surface, giving a UV-Vis signal above 240 nm. The second one, whose binding energy was between those of TiO$_2$ and TS-1, was representative of isolated tetrahedrally coordinated Ti(IV) species. The inhomogeneity in Ti dispersion of the surface of the sample was also confirmed by a quantitative evaluation of the Ti/Si ratio by XPS. This ratio (0.02) was very close to that obtained by chemical analysis (0.018). If titanium was highly dispersed on the silica surface, we would expect a higher value for the Ti/Si ratio by XPS than by chemical analysis. The similarity between ratios obtained by both methods can be explained by the presence of small TiO$_2$ particles on the surface of the material. However, an EDX examination of the solid confirmed that the size of these TiO$_2$ nanodomains did not exceed a few nanometers. With a 15-nm diameter probe, an average Ti content of 2.9 wt% was found and individual determinations never exceeded 4 wt% Ti. This shows that even though large TiO$_2$ particles were not present on the silica surface, the distribution of Ti species was not uniform. For comparison, the same analysis performed on titanium silicalite-1 (TS-1) gave 1.5 wt% Ti with a maximum dispersion of ±0.2 wt%.

As for samples prepared in diglyme, we have examined the influence of an acid treatment (HNO$_3$, 6 M) on calcined solids prepared at different pH values (Table 3). For samples prepared at pH < 8, more than 70% of titanium is leached upon the treatment, which means that Ti species are weakly bonded to the silica surface. This percentage decreases to about 50% for the last sample prepared at pH = 10. Whilst UV-Vis spectra of untreated materials were more or less similar, very important differences are observed for washed samples (Fig. 3). Samples prepared at pH < 6 show a very broad absorption at 270 nm with an absorption edge at about 370–380 nm. The spectra of samples synthesized at pH > 8 show a narrow absorption band at 225 nm, characteristic of isolated, tetrahedrally coordinated Ti species, without any signal above 310 nm. The sample prepared at pH = 6 shows an intermediate situation, with signals at 230 and 300 nm. Therefore, it seems that basic conditions are necessary to have a strong attachment of titanium on the silica surface when the reaction is performed in water. Indeed, under these conditions, hydrolysis of Ti−F bonds and condensation with silanol groups of silica are greatly favored. The UV-Vis spectrum of the sample prepared at pH = 10, washed with nitric acid and subsequently dried in a vacuum is very similar to that of TS-1 samples, which suggests that all Ti species are isolated and tetrahedrally coordinated. In fact, the position and width of the absorption band strongly depend on the degree of hydration of the sample. Hydration shifts the maximum to 240 nm and drastically broadens the line, giving a signal similar to that of the untreated sample. The process is totally reversible and a narrow absorption at ca 220 nm is recovered upon outgasing the sample at 200°C. Similar observations have been reported by Klein *et al.* (30) on Ti−Si mixed oxides. We have already mentioned that the Ti2p3/2 XPS line of the unwashed sample could be deconvoluted into two components corresponding to isolated Ti species and TiO$_2$ domains, respectively. After washing by nitric acid, the position of the line is shifted to 459.3 eV, which suggests that the acid treatment preferentially removed TiO$_2$ nanoparticles (Fig. 4). This is in agreement with UV-Vis data and it was confirmed by EDX analysis of the silica surface.

1.2. Influence of the Ti content. We have also examined the influence of the Ti content on the dispersion of the species on the surface of the support. A series of samples has been prepared at pH = 10 following Method 2 of the Experimental section, in which the amount of titanium was increased from 0.5 to 8 wt%. For all samples, 80 to 90% of the titanium originally introduced in the synthesis mixture was fixed on the silica surface (Table 4). For low loadings, the amount of fluorine on the solid is low but it increases with the Ti content. The UV-Vis spectra of the samples show an increase in the intensity of the absorption band, together with a shift of the maximum absorption towards low energies with the Ti content. The position of

TABLE 4

Ti and F Contents (wt%) in Samples Prepared with Various Amounts of TiF$_4$ and Percentage of Ti Retained on the Silica Surface

Ti (wt%) introduced	0.5	1	2	3	4	6	8
Ti (wt%)	0.45	0.90	1.78	2.75	3.44	4.97	6.56
F (wt%)	0.24	0.25	0.25	0.95	1.28	1.89	1.88
Percentage of Ti on silica	90	90	89	92	86	83	82

the maximum of absorption increases almost linearly up to 5 wt% Ti and then remains constant at ca 270 nm for higher loadings (Fig. 5). In fact, each UV-Vis spectrum can be interpreted as the superposition of one absorption at 220 nm, due to isolated Ti species, one absorption around 270 nm attributed to small TiO$_2$ particles and an additional signal above 300 nm assigned to large TiO$_2$ domains. The relative populations of the two first species can be estimated by measuring the intensities of the absorptions at 220 and 270 nm in the UV spectra. Up to about 3 wt% Ti in the samples, isolated Ti species predominate (Fig. 5). Above 3 wt% Ti, the number of isolated Ti(IV) species remains almost constant whilst the contribution of TiO$_2$ nanoparticles still increases. Thus, for high loadings, the formation of Ti–O–Ti bridges seems to be detrimental to the incorporation of titanium species in the silica framework. Similar conclusions were obtained from the study of the optical density of the band at 960 cm^{-1} observed in the IR spectra of the samples. It has been widely reported that the intensity of this band could be correlated with the number of Si–O–Ti bridges in titanium-containing zeolites. This correlation is not so evident on amorphous solids, where this band is also observed on pure silica materials, due to the presence of surface silanol groups. However, up to about 3 wt% Ti in the samples, we observed a linear increase of the optical density of the IR band at 960 cm^{-1} with the Ti content. For higher loadings, a deviation was observed, in agreement with UV-Vis data which indicated the preferential formation of Ti–O–Ti bonds. The presence of large TiO$_2$ particles in samples with high Ti loadings was also confirmed by EDX. In some regions of the silica surface, Ti/Si ratios higher than 0.7 have been measured.

1.3. Acidity of the materials. SiO$_2$–TiO$_2$ mixed oxides are known to possess an acidity which is usually different from that of pure oxides SiO$_2$ and TiO$_2$ (33–37). Whilst the acidity of pure SiO$_2$ can be considered as negligible, that of TiO$_2$ is essentially due to Lewis sites. The observation of Brönsted sites in TiO$_2$ is generally due to impurities, mostly SiO$_2$. Most of SiO$_2$–TiO$_2$ mixed oxides possess Brönsted and Lewis acid sites (33–37). It is usually observed that the number of Brönsted sites varies with the Ti/Si ratio and that the Lewis acidity depends on the dispersion and coordination of titanium as well as on the Ti content. It is expected that no Brönsted acidity is detected in solids where titanium atoms are perfectly isolated and tetrahedrally coordinated. However, these samples possess a Lewis acidity, due to the uncompleted coordination of Ti atoms, as was already observed for TS-1 (38). In contrast, if small TiO$_2$ particles are present, Brönsted sites may exist at the interface between SiO$_2$ and TiO$_2$, and their number and strength strongly depend on the nature of the interface.

After adsorption of pyridine on pure silica FK 310 and subsequent evacuation at 50°C, bands at 1596, 1580, 1490, and 1445 cm^{-1} are observed in the IR spectrum. These bands can be assigned to different vibration modes of pyridine in the gas phase (1580, 1490, and 1440 cm^{-1}) and pyridine in interaction with silanol groups of the silica surface (1596 and 1445 cm^{-1}). When the same experiment is performed on a sample containing approximately 1 wt% Ti, a new absorption band is observed at 1607 cm^{-1}, which

FIG. 5. Maximum UV/Vis absorption (a) and relative intensities of the absorptions at 220 nm (□) and 270 nm (■) with the Ti content for Ti/SiO$_2$ materials.

corresponds to the vibration mode [8a] of pyridine adsorbed on Lewis acid sites. For this sample, no significant band is detected around 1545 cm^{-1}, which confirms the absence of Brönsted sites. As we have previously mentioned, the presence of Lewis centers in the sample may result from isolated, tetrahedrally coordinated Ti(IV) species in the silica matrix or from small TiO$_2$ particles. Indeed, a mechanical mixture of FK 310 and TiO$_2$ gives a very weak signal around 1605 cm^{-1}. Thus, the presence of TiO$_2$ alone cannot explain such a high amount of Lewis acid centers and the only possibility is to consider that the major part of Ti atoms are isolated in the silica framework in a tetrahedral environment.

The evolution of the number of Lewis sites with the Ti loading can be estimated from the area of the IR absorption band at 1607 cm^{-1}. We observe that the area of the band increases rapidly up to a Ti content of about 3 wt% and then slowly for higher loadings (Fig. 6). Above 3 wt% Ti in the samples, addition of titanium does not drastically modify the Lewis acidity of the solids. This is likely due to the formation of relatively large TiO$_2$ particles, since we have seen that the acidity of TiO$_2$ was negligible compared to that of isolated titanium species or TiO$_2$ nanodomains. The formation of large TiO$_2$ particles is in agreement with our previous observations which suggested the preferential formation of Ti–O–Ti bonds above ca 3 wt% Ti in the samples. If we compare now IR results with UV-Vis data, the amount of Lewis acid sites can be directly correlated neither with the intensity of the absorption band at 220 nm nor with the intensity of the absorption at 270 nm. However, we found an excellent correlation between the number of Lewis centers and the sum of the UV-Vis intensities at 220 and 270 nm, which correspond to isolated Ti(IV) species and TiO$_2$ nanodomains, respectively (Fig. 6). This is additional evidence
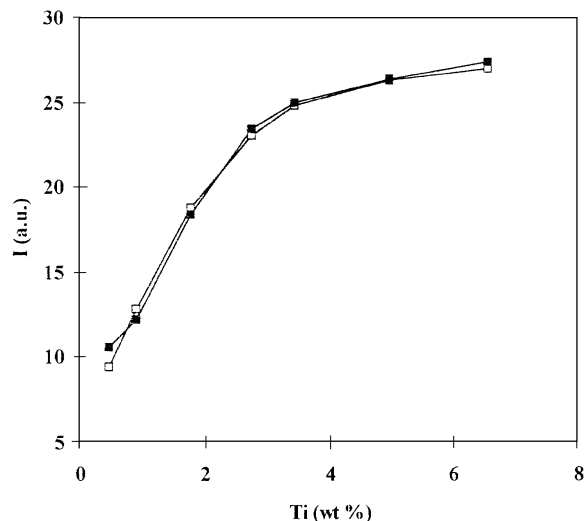
that TiO$_2$ nanodomains can possess a Lewis acidity, which is impossible to differentiate from that of isolated Ti(IV) species by means of pyridine adsorption. Above 3 wt% Ti, the lower increase in both IR and UV intensities could be explained by the formation of large TiO$_2$ particles. These particles posses a very low amount of Lewis sites and are responsible of the increase in the UV-Vis absorption edge at high Ti loadings. Simultaneously, increasing the Ti loading results in the appearance of Brönsted acid centers, characterized by an infra red absorption for pyridine at 1545 cm^{-1}. These sites probably exist at the interface between TiO$_2$ nanodomains and silica, but their number is always small compared to that of Lewis sites.

2. Catalytic Properties

2.1. Nature of the products formed. The catalytic oxidation of cyclohexene has been carried out over Ti/SiO$_2$ materials prepared at pH = 10 following Method 2 of the Experimental section. Indeed, this method has the advantage of providing directly defluorinated solids whose physical properties are similar to those of solids obtained in an organic solvent after ammonia treatment. When not specified, catalysts contained about 1.5 wt% Ti and the reactions were performed as reported in the experimental section, i.e. with 1 g of catalyst, 250 mmol of cyclohexene, and 11 mmol of oxidant.
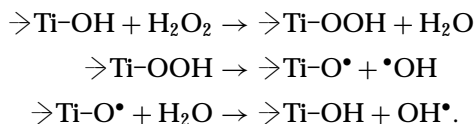
Ti/SiO$_2$ systems are known to catalyze the epoxidation of olefins with organic hydroperoxides (1, 6–11, 23). Therefore, we have first checked that our materials were active in the epoxidation of cyclohexene with anhydrous *tert*-butyl hydroperoxide (TBHP, 95 wt% in cyclohexane). After 3 h reaction at 90°C, all TBHP was consumed and cyclohexene oxide was the only product formed with a selectivity of 96% with respect to the oxidant. This proves that the synthesized solids are very active in this reaction and that the substrate is converted to cyclohexene oxide by a nonradical mechanism (direct epoxidation).

When H$_2$O$_2$ (70 wt% in water) is used as the oxidant, the nature and selectivities of the products formed are very different. After 4 h reaction, four products are detected by gas chromatography, namely cyclohexene oxide, cyclohexanediol, 2-cyclohexene-1-ol (cyclohexenol), and 2-cyclohexene-1-one (cyclohexenone). As shown in Fig. 7a, the amount of cyclohexenone increases very rapidly after the addition of H$_2$O$_2$ and then slowly decreases with reaction time. Simultaneously, cyclohexene oxide and the alcohol are formed in similar amounts and their selectivity reaches approximately 41% after 4 h. Cyclohexanediol is also formed, but in very small amounts, compared to the epoxide and alcohol. Plotting the amount of products formed as a function of the substrate conversion immediately shows that the ketone is a primary product of the reaction (Fig. 7b). On the other hand, cyclohexene oxide and cyclohexenol seem to be essentially secondary products,

FIG. 6. Total UV/Vis intensity ($I_{220} + I_{270}$) (□) and area of the pyridine absorption band at 1607 cm^{-1} (■) as a function of the Ti content.

whose formation is related to the consumption of cyclohexenone. However, the production of similar amounts of alcohol and epoxide from a ketone is quite unexpected under the reaction conditions.

As large amounts of allylic oxidation products are detected in the reaction mixture, the mechanism probably involves radicals. These radicals come from the decomposition of peroxo titanium species formed by reaction of H_2O_2 with the titanium sites of the catalyst:

Initiation,

$$\rightarrow Ti\text{-}OH + H_2O_2 \rightarrow\ \rightarrow Ti\text{-}OOH + H_2O$$

$$\rightarrow Ti\text{-}OOH \rightarrow\ \rightarrow Ti\text{-}O^\bullet + {}^\bullet OH$$

$$\rightarrow Ti\text{-}O^\bullet + H_2O \rightarrow\ \rightarrow Ti\text{-}OH + OH^\bullet.$$
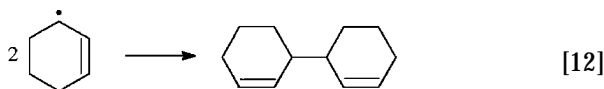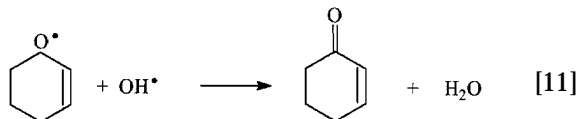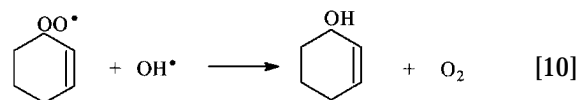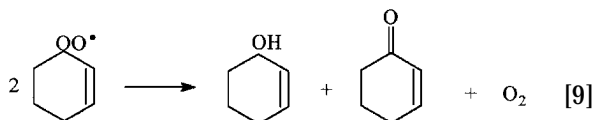
These radicals can further react with the substrate following the reactions:

*Propagation,*

[5]

[6]

[7]

[8]

Termination,

[9]

[10]

[11]

[12]
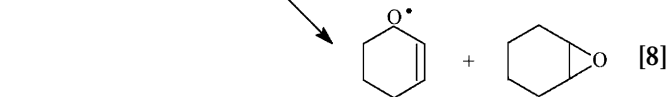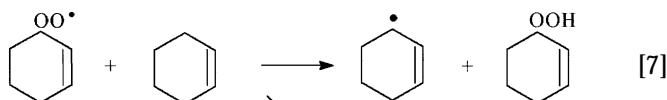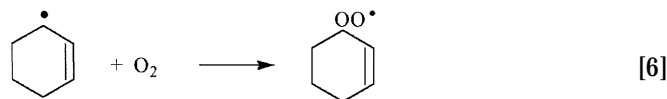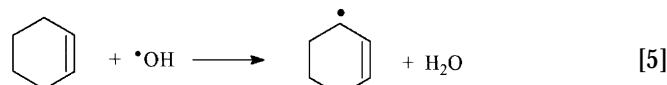
Therefore, a radical mechanism can account for the presence of cyclohexene oxide, cyclohexenol, and cyclohexenone in the reaction mixture. However, none of these reactions can explained why the ketone is consumed with time and why epoxide and alcohol are formed in equal amounts.

The simultaneous formation of equal amounts of cyclohexene epoxide and cyclohexenol has already been observed in homogeneous catalysis by transition metal complexes (Mo, V, etc.). Some authors have reported the formation of cyclohexenyl hydroperoxide (CHHP) following reactions [5], [6], and [7] and its subsequent reaction with cyclohexene (39):

[13]
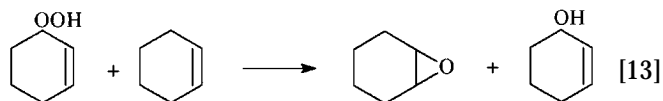
Following this scheme, cyclohexene oxide and cyclohexenol are formed in equal amounts, which strongly suggests that CHHP could be involved in the epoxidation of cyclohexene with H_2O_2 over Ti/SiO$_2$ materials. Moreover, Lempers *et al.* (40) have shown that CHHP undergoes rapid decomposition at 80°C over transition metal-containing molecular sieves like CrAPO$_4$-5, yielding cyclohexenol and cyclohexenone in a ratio of about 30 : 70. Therefore, the formation of CHHP could also account for the presence of the ketone in the products. However, if cyclohexenone is formed by decomposition of CHHP over the catalyst, we would not expect its concentration to decrease with the reaction time. Another possibility to explain the presence of cyclohexenone is to suppose that it is formed by decomposition of CHHP in the injector of the chromatograph. Under such conditions, the amount of ketone is directly proportional to that of peroxide and decreases with reaction time according to reaction [13]. In order to check this assumption, we have prepared a solution of CHHP in cyclohexene following a recipe given by Lempers *et al.* (40). After injection of the solution in the chromatograph, cyclohexenone and cyclohexenol were detected in a ratio of about 4 : 1, not very different from that obtained after decomposition of CHHP over CrAPO$_4$-5.

We can thus conclude that cyclohexenone detected by gas chromatography essentially results from the decomposition of CHHP at high temperature. Small amounts may also be produced by reaction [11], but generation of
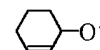
radicals would lead to an excess of epoxide with respect to cyclohexenol (reaction [8]), which is not observed experimentally. Under these conditions, it is possible to estimate

the concentration in CHHP in the reaction mixture by measuring the amount of cyclohexenone formed:

$$[CHHP] \approx [cyclohexenone]/0.8. \qquad [14]$$

We have performed a reaction in which CHHP was used as oxidizing agent instead of H_2O_2. The evolution of the products formed during reaction shows that CHHP is consumed with time and leads to the formation of epoxide and alcohol. Note that no reaction occurs in the absence of a catalyst; the solution of CHHP is stable for several hour at $90°C$. Data are very similar to those of Fig. 7, which confirms that CHHP is certainly the oxygen source in the reaction. A small excess of alcohol is observed, due to either termination reactions like [10] or to a change in the ketone/alcohol
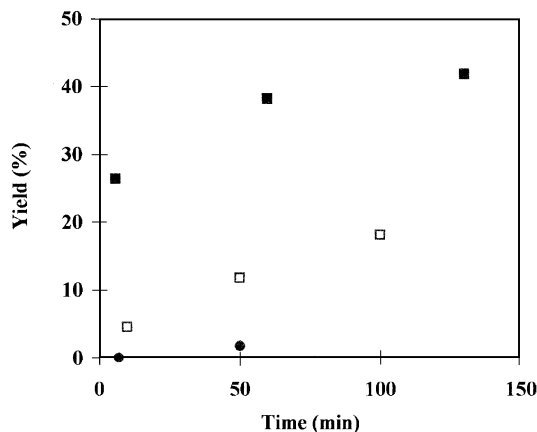
a

b

FIG. 7. Yields of products formed relative to initial H_2O_2 as a function of time (a) and substrate conversion (b) during the oxidation of cyclohexene over Ti/SiO$_2$ materials. ($\blacklozenge$), O$_2$; ($\blacksquare$), cyclohexene oxide; ($\square$), cyclohexenol; ($\bullet$), cyclohexenone; and ($\circ$), cyclohexanediol. Reaction conditions: 1 g catalyst, 250 mmol cyclohexene, 11 mmol H_2O_2, T = $90°C$.

FIG. 8. Cumulated yield of CHHP relative to initial H_2O_2 formed over Ti/SiO$_2$ ($\blacksquare$), silica FK 310 ($\square$), and without solid ($\bullet$).

ratio obtained by decomposition of CHHP in the injector with reaction time.

2.2. Formation of cyclohexene hydroperoxide over Ti/ SiO$_2$ catalysts. As already mentioned, the formation of CHHP necessitates the presence of radicals, generated by reaction between H_2O_2 and the titanium sites of the catalyst. Assuming that the ketone formed results essentially from the decomposition of CHHP in the chromatograph, it is possible to estimate the cumulated amount of peroxide formed during the catalytic reaction. As shown in Fig. 8, only traces of CHHP are formed in the absence of a catalyst. Over pure silica FK 310, a small amount of CHHP is formed, probably because of the presence of impurities in the silica (mostly Fe$_2$O$_3$). Without a catalyst, as well as over pure silica, CHHP is very stable and no oxidation products are formed. Over Ti/SiO$_2$, the initial rate of formation of CHHP is very high, but the hydroperoxide is immediately consumed following reaction [9]. Moreover, when H_2O_2 is introduced in the reaction mixture in one lot, it is partially decomposed to oxygen (Fig. 7) or used for the nonradical epoxidation of cyclohexene, which causes the amount of CHHP formed to be usually smaller than that of H_2O_2 introduced.

2.3. Role of molecular oxygen. Reaction [6] shows that the formation of CHHP can also be initiated by oxygen. An experiment performed under an oxygen flow (20 ml/min) shows that the total amount of products formed is approximately three times higher than in the absence of O$_2$. At the end of the reaction, the total yield of products with respect to H_2O_2 initially introduced is close to 300%, which clearly demonstrates the role of oxygen in the catalytic process. The evolution of the amount of CHHP in the reaction mixture with time is reported in Fig. 9. During the first minutes following addition of H_2O_2, the rapid formation of CHHP corresponds to the consumption of hydrogen peroxide. Then the formation stops and the amount of CHHP
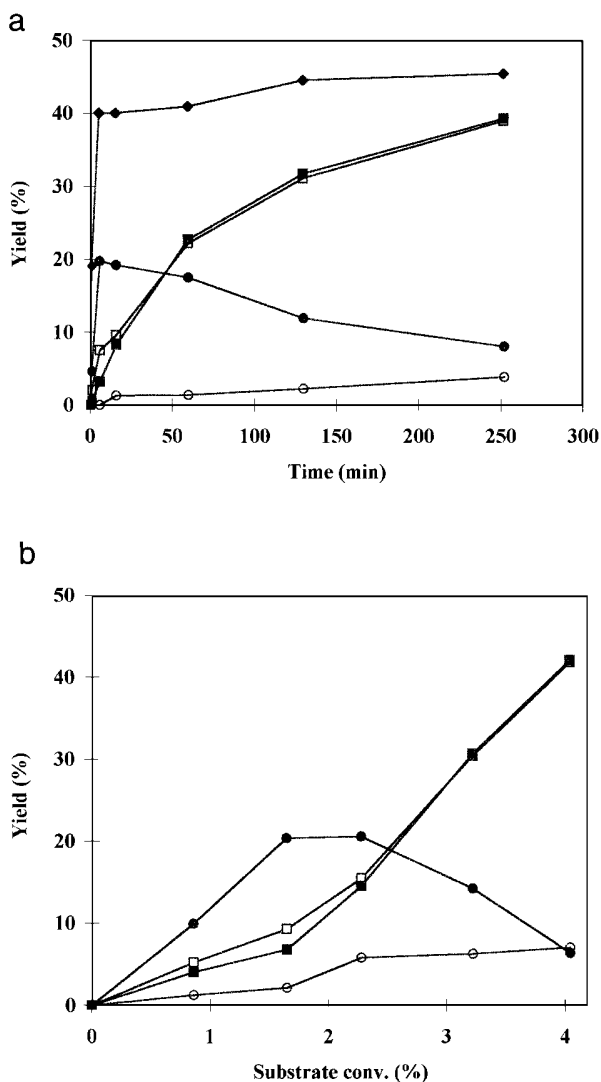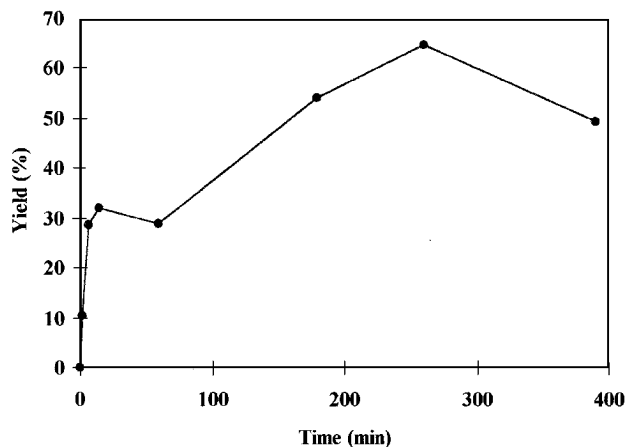
FIG. 9. Evolution of the yield of CHHP relative to initial H_2O_2 during the epoxidation of cyclohexene with H_2O_2 under oxygen flow.

even slightly decreases due to reaction [13]. After about 60 min, we observe that the amount of CHHP increases again due to reaction [6], which is not observed in the absence of oxygen. Concerning the nature and selectivities of the products formed, they are the same as in the absence of oxygen, but the amounts of epoxide and alcohol are about three times larger.

2.4. Nonradical versus radical mechanisms. We have shown that the formation of cyclohexene oxide and cyclohexenol could be explained by a mechanism involving radicals. However, a small amount of epoxide might also be obtained by a direct epoxidation route in the absence of radicals:

$$\text{>Ti-O-O-H} \; + \; \bigcirc \; \longrightarrow \; \text{>Ti-OH} \; + \; \bigcirc\!\!\!\!O$$

$$[15]$$

However, as the epoxide and alcohol are formed in very similar amounts, the amount of epoxide formed by direct epoxidation following reaction [15] is probably small. Assuming that the decomposition of CHHP into cyclohexenol and oxygen is negligible, the amount of epoxide formed by the radical mechanism is equal to that of alcohol (reaction [13]). Thus the amount of cyclohexene oxide formed by direct epoxidation is obtained by the difference between the total amount of epoxide and the amount of alcohol. Figure 10 shows the formation of the different products, taking into account the epoxide formed by direct epoxidation. As expected, epoxide formed following reaction [15] represents only 12% of the epoxide formed. During the first minutes following addition of H_2O_2, about 75% of the total oxidant ($H_2O_2 + $ CHHP) is consumed. In fact, most of H_2O_2 is decomposed to give oxygen and CHHP. A small fraction of H_2O_2 is used for the direct epoxidation of cyclohexene but the reaction stops when hydrogen peroxide has

been totally consumed. After about 15 min, the amount of epoxide formed by direct epoxidation is constant and even slightly decreases due to the ring opening and the formation of cyclohexanediol. Simultaneously, CHHP starts to be consumed, and cyclohexene oxide and cyclohexenol are formed by reaction [13].

As will be discussed in the next subsection, the direct epoxidation of cyclohexene is very sensitive to the presence of water in the reaction mixture. Experiments performed with dropwise addition of the oxidizing agent considerably increases the amount of cyclohexene oxide formed by the nonradical mechanism.

2.5. Influence of water. Many authors have reported that Ti/SiO_2 catalysts, as well as Ti–Si mixed oxides are not active in the epoxidation of olefins with aqueous H_2O_2 due to the hydrophilic character of their surface, compared to zeolites. It is the reason why we have performed most of our experiments with relatively concentrated hydrogen peroxide solutions (70 wt% in water). In order to evaluate the influence of water on the catalytic process, a reaction has been carried out with the same H_2O_2/cyclohexene ratio but using a 30 wt% hydrogen peroxide solution. Results are summarized in Fig. 11. As with a 70 wt% H_2O_2 solution, CHHP is rapidly formed upon addition of hydrogen peroxide. However, after about 15 min, the amount of CHHP remains constant and does not decrease as it is observed with concentrated solutions. This suggests that reaction [13] is drastically inhibited by the presence of an excess of water in the reaction mixture. As a consequence, the amounts of epoxide and alcohol formed are low. Moreover, these amounts are strictly the same and no epoxide is formed by the direct nonradical route. In order to confirm that water
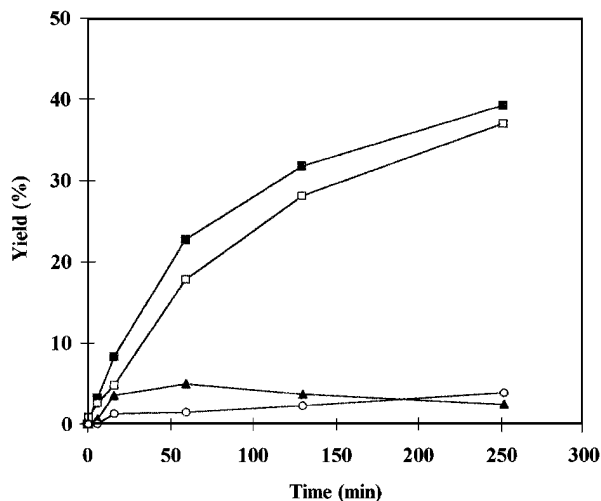

FIG. 10. Yield of products formed relative to initial H_2O_2 during the epoxidation of cyclohexene with H_2O_2: (■), total cyclohexene oxide; (□), cyclohexenol; (○), cyclohexanediol; and (▲), cyclohexene oxide obtained by direct epoxidation.
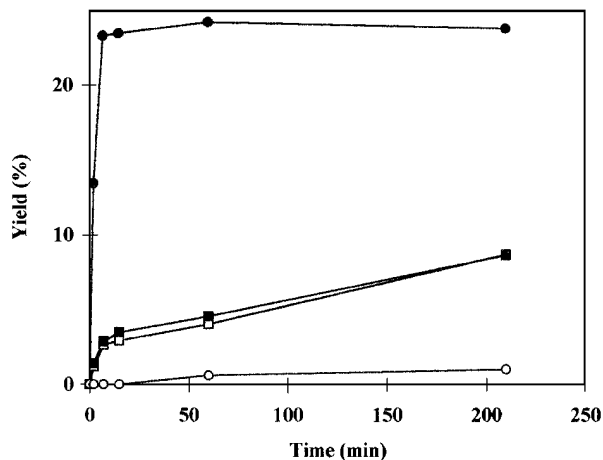
FIG. 11. Yield of products formed relative to initial H_2O_2 during the epoxidation of cyclohexene with diluted H_2O_2 (30 wt% in water): (●), O_2; (■), cyclohexene oxide; (□), cyclohexenol; and (○), cyclohexanediol.

is responsible for the decrease in activity of the catalysts, an experiment has been performed with concentrated H_2O_2 but with adding the amount of water equivalent to that introduced using a 30 wt% solution. The results are strictly similar to those of Fig. 11, which proves that water blocks the catalytic process. Interestingly, the formation of CHHP is not affected by the presence of water in the reaction mixture, indicating that peroxo titanium species can be formed in an excess of water and undergo decomposition to give the radicals.

As a corollary to the above, we expect an increase in the catalytic activity of Ti/SiO_2 systems by decreasing the concentration of water. An experiment has thus been carried out by adding H_2O_2 (70 wt%) dropwise over 1 h, instead of in one lot. Such conditions do not exactly correspond to an experiment performed with a lower water concentration, since the amount of water at the end of the addition of the oxidant is the same as that introduced when H_2O_2 is added in one lot. However, only traces of water are present at the beginning of the reaction, which should affect the final selectivities. Three hours after the complete addition of H_2O_2, cyclohexene oxide is the major product formed with a selectivity of about 84% with respect to hydrogen peroxide (Table 5). In contrast to reactions in which H_2O_2 is added in one lot, the amount of cyclohexenol is low, which

shows that the major part of cyclohexene oxide is formed by a nonradical mechanism. Since the total yield of products relative to initial H_2O_2 is 126%, this indicates that cyclohexenol and part of cyclohexene oxide are formed by a radical process and that oxygen must play a role as the oxidizing agent.

In conclusion, experimental data tend to show that water blocks the catalytic sites responsible for the epoxidation of cyclohexene by both the nonradical and radical pathways. The direct epoxidation is only possible when very low amounts of water are present, in agreement with results obtained over titanium-substituted zeolites. Indeed, the excellent performance of TS-1 in the epoxidation of linear olefins has been attributed to its hydrophobic character, thus isolating catalytic sites from water. Water also inhibits the production of epoxide and alcohol by reaction [13], but to a lower extent than for the direct epoxidation. Actually this does not result from changes in the amount of CHHP formed. Indeed, water has a very small influence on the production of radicals by decomposition of peroxo titanium species, and CHHP is formed in similar amounts with concentrated or diluted H_2O_2 solutions.

2.6. Influence of the calcination of the catalysts. As shown in Fig. 12, cyclohexene oxide is formed in higher amounts when the catalyst has been calcined at 500°C prior to the catalytic test. This was not observed over as-synthesized catalysts where the amounts of epoxide and alcohol formed were similar, indicating that direct epoxidation did not occur. Moreover, the difference observed between cyclohexene oxide and cyclohexenol suggests that about 33%
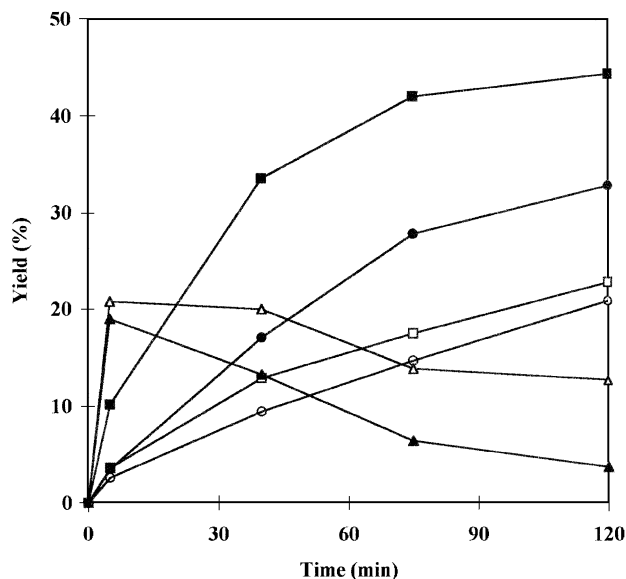
TABLE 5

Epoxidation of Cyclohexene over Ti/SiO₂ with H₂O₂ (70 wt%) Added over 1 h

Ti (wt%)	H₂O₂ conversion (%)	Selectivity/H₂O₂ (%)			
		Epoxide	Diol	Alcohol	CHHP
1.4	100	84	14	25	3

FIG. 12. Yield of products formed relative to initial H_2O_2 during the epoxidation of cyclohexene with H_2O_2 over as-synthesized (white symbols) and calcined (black symbols) Ti/SiO_2 catalysts: (■, □), cyclohexene oxide; (●, ○), cyclohexenol; and (▲, △), CHHP.

of epoxide is formed by a nonradical route. The amount of CHHP formed is the same over as-synthesized and calcined catalysts, but the evolution with time shows that the calcined material is more active in reaction [13]. The increase in activity upon calcination for both the nonradical and radical routes probably results from an increase in the hydrophobic character of the material, due to silanol condensation at high temperature. We also observe that cyclohexanediol is formed in larger amounts over calcined catalysts. It is usually reported that cyclohexanediol results from the hydrolysis of cyclohexene oxide in the presence of acid sites. In as-synthesized samples, these sites could be neutralized by traces of ammonia resulting from the preparation, and they could be regenerated upon calcination at 500°C. The presence of traces of ammonia could also explained why as-synthesized samples are less active than calcined samples in the epoxidation of cyclohexene.

2.7. Influence of the Ti content. We have performed a series of catalytic tests over Ti/SiO$_2$ materials containing increasing amounts of titanium, typically from 0.5 to 6.5 wt%. In order to obtain higher activities, the solids were calcined at 500°C prior to catalytic tests. We have first measured the specific activity for the different products, i.e. the rate of formation of these products per minute and per gram of titanium as a function of the Ti content. Rates of formation have been measured by analyzing the solution one minute after addition of H$_2$O$_2$ (in one lot). Under these conditions, we have considered that cyclohexenol detected by GC results only from the decomposition of CHHP in the injector. At 0.5 wt% Ti, only CHHP is formed and the epoxide is not detected (Fig. 13). Up to 2 wt% Ti, the specific activity in epoxidation increases with the Ti content, and then decreases for higher Ti contents. No cyclohexanediol is formed with samples containing less than 1 wt% Ti.
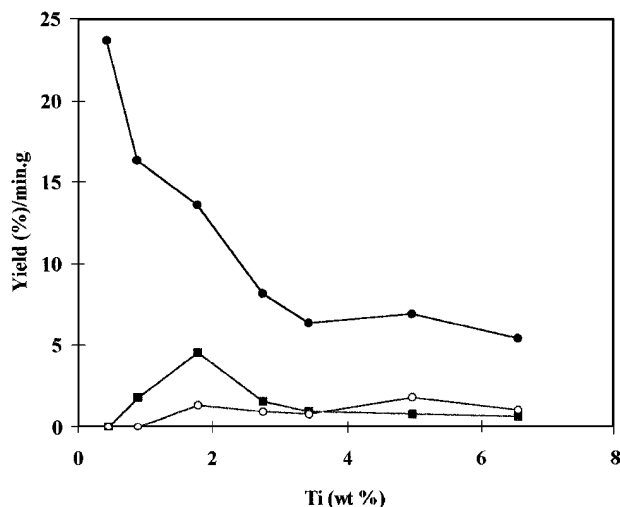

FIG. 13. Specific activity of the catalysts in (●), CHHP; (■), cyclohexene oxide; and (○), cyclohexane diol with the Ti content in the samples.

TABLE 6

Epoxidation of Cyclohexene with H$_2$O$_2$ (70 wt%) over Ti/SiO$_2$ with Various Ti Contents

Ti (wt%)	Selectivity (%)/H$_2$O$_2$				
	Epoxide	CHHP	Alcohol	Diol	Total
0.45	24	16	20	1	61
0.9	32	11	26	2	71
1.78	26	4	27	21	78
2.75	19	4	26	29	78
3.44	11	4	24	32	71
4.97	4	3	21	37	65
6.56	5	4	22	34	65
4.3[a]	7	5	14	21	47

[a] TiO$_2$–SiO$_2$ mixed oxide (Grace, 4.3 wt% Ti, 460 m^2/g).

For higher loadings, the activity first increases between 1 and 2 wt%, and then remains constant, suggesting that the sites responsible of the formation of cyclohexanediol are not modified between 2 and 6.5 wt%.

The specific activity in CHHP decreases with the metal content between 0.5 and 3 wt% and then remains constant for higher loadings (Fig. 13). It seems therefore that the addition of titanium strongly modifies the catalytic performance of the materials, particularly for Ti contents in the range of 0.5–3 wt%. The differences between the various catalysts are also clearly evidenced by comparing the product selectivities after the 3.5-h reaction (Table 6). For all catalytic runs, the total product selectivity with respect to H$_2$O$_2$ is lower than 100% due to partial decomposition of the peroxide immediately after addition. For low Ti contents, CHHP is still present at the end of the reaction, which indicates that reaction [13] is catalyzed by Ti species and confirms the absence of reaction over pure silica FK 310. Concerning the products formed, very important variations are observed in epoxide and diol selectivities with the Ti content. Results show that sites capable of transforming cyclohexene oxide to cyclohexanediol are formed at high Ti loadings. For a sample with 6.56 wt% Ti, almost 85% of the epoxide has been converted into diol after the 3.5-h reaction. These sites are probably Brönsted centers, since we have shown by pyridine absorption that the number of Brönsted sites increased with the Ti content when catalysts contain more than 1.5 wt% Ti.

Concerning cyclohexene oxide, the specific activity increases rapidly with the Ti content up to about 2 wt% and then decreases for higher Ti contents. The maximum in activity corresponds to the maximum number of Lewis sites per gram of titanium, which strongly suggests that epoxidation is catalyzed by Lewis sites (Fig. 14). As we have previously discussed, these sites could arise from isolated Ti(IV) species or TiO$_2$ nanodomains at the surface of the silica. Moreover, Fig. 14 confirms that above 2 wt% Ti, large
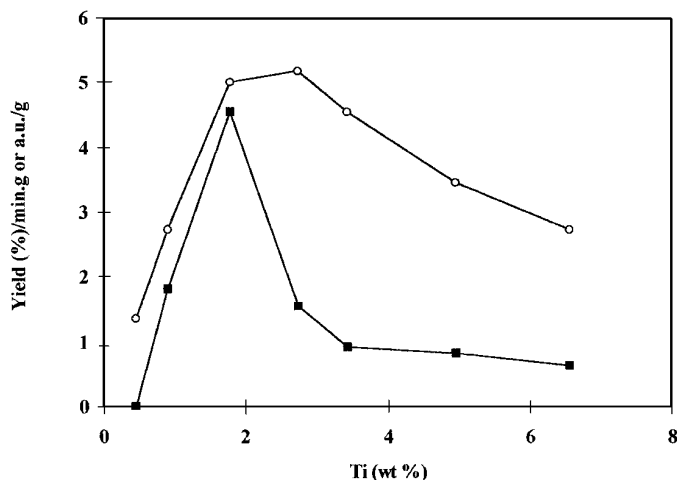
FIG. 14. Specific activity of the catalysts in cyclohexene oxide (■) and area of the pyridine IR absorption band at 1607 cm^{-1} (○) with the Ti content in the samples.

TiO_2 particles, which do not possess Lewis acidity, are preferentially formed. Figure 15 shows that the initial rate of formation of CHHP increases with the Ti content, but that the specific activity per gram of Ti decreases monotonously from 0.5 to about 4 wt% Ti. Similar observations have been reported by Klein *et al.* (10) in the catalytic oxidation of 1-octene with TBHP over Ti–Si mixed oxides. The decrease in initial turnover frequency with the Ti content was attributed to diffusion limitations due to the small pore size of the materials (typically 0.7–0.8 nm). A correlation between the initial rate of cyclohexene epoxidation and the mean pore diameter of aerogels has also been observed by Dutoit *et al.* (11). As our starting silica FK 310 possesses micropores in the 0.8–2 nm range, diffusion limitations could
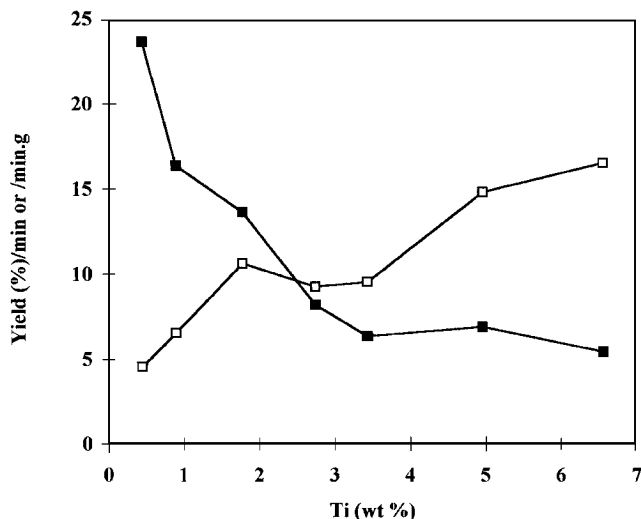

FIG. 15. Initial rate of formation (yield/min) (□) and specific activity (yield/min · g) (■) of CHHP with the Ti content in the samples.

also explain the decrease in the initial rate of formation of CHHP with the Ti content. Comparison with Fig. 14 suggests that the formation of CHHP and cyclohexene oxide by reaction [13] occur on the same catalytic sites. From 0.5 to 2 wt% Ti, addition of Ti favors the formation of epoxide and, thus, sites are less available for the production of CHHP. For higher Ti loadings, both reactions are inhibited, resulting from the covering of the silica surface by relatively large TiO_2 particles. Catalysts possessing more than 4 wt% Ti behave like Ti–Si mixed oxides; an experiment performed over a mixed oxide (Grace, 4.3 wt% Ti) gives very similar selectivities (Table 6).

IV. CONCLUSION

Ti-grafted SiO_2 materials have been prepared at low temperature from the reaction of TiF_4 with silica in the liquid phase. The materials can be synthesized either in an organic solvent (diglyme) or in water. When diglyme is used as the solvent, all Ti and F originally introduced in the reaction mixture are fixed on the silica surface but spectroscopic data show that Ti is partially defluorinated and that Si–F bonds are formed. All fluorine can be removed by washing the solids with an aqueous solution of ammonia, which affects neither the Ti content nor the dispersion of metal species on the silica surface. A subsequent calcination at 500°C reinforces the fixation of Ti species to silica, probably by condensation of the titanol and silanol groups.

When Ti/SiO_2 materials are prepared in water, the amount of Ti fixed on the silica depends on the pH of the solution and high Ti loadings can only be obtained at pH >8. Moreover, the interaction between titanium and silica is weak for samples prepared at low pH values and most of Ti species are removed upon an acid washing. From a spectroscopic point of view, samples prepared at pH = 10 are similar to those synthesized in diglyme after treatment with ammonia. However, the use of water has the advantage that samples are directly defluorinated, which does not necessitate a two-step preparation method.

For Ti contents lower than about 2.5 wt%, most Ti atoms are directly bonded to the silica surface but spectroscopic data do not exclude the presence of small TiO_2 nanodomains. Samples possess exclusively Lewis acid sites, whose number is proportional to the Ti content. These Lewis centers result from the presence in the material of isolated tetrahedrally coordinated Ti(IV) species or TiO_2 nanodomains in which most of Ti atoms are directly bonded to the silica.

With increasing the Ti content, Ti–O–Ti bonds are preferentially formed and the titanium species possess all the characteristics of TiO_2. In particular, the number of Lewis centers remains approximately constant whilst Brönsted acid sites are observed. Therefore, it seems that high Ti dispersions can only be obtained for Ti loadings lower than

about 2.5 wt% Ti, which could correspond to the complete coverage of the surface of the silica particles.

These materials catalyze the epoxidation of cyclohexene with concentrated aqueous H_2O_2 solutions. This oxidizing agent leads to the formation of allylic oxidation products like cyclohexenyl hydroperoxide and 2-cyclohexene-1-ol, in addition to cyclohexene epoxide and cyclohexanediol, which are the only products obtained with anhydrous TBHP. Cyclohexenyl hydroperoxide is formed immediately after the addition of hydrogen peroxide by a radical mechanism and further reacts with cyclohexene to give epoxide and alcohol in similar amounts. A small fraction of H_2O_2 initially introduced is also used for the direct nonradical epoxidation of cyclohexene and gives exclusively the epoxide.

Oxygen plays an important role in the reaction, particularly on the formation of cyclohexenyl hydroperoxide, which causes the total amount of products formed usually to exceed that of the H_2O_2 initially introduced when the reaction is performed under an oxygen flow. Increasing the Ti content in the catalysts up to about 2.5 wt% increases the specific activity in epoxidation. Beyond this value, large amounts of cyclohexanediol are formed, due to the presence of Brönsted acid centers in the materials.

Whilst CHHP is also formed when diluted H_2O_2 solutions are used, both the direct epoxidation and the bimolecular reaction between CHHP and cyclohexene yielding epoxide and cyclohexenol are inhibited by an excess of water. On the contrary, when concentrated H_2O_2 is added dropwise, the direct epoxidation route is favored and cyclohexene oxide is the major product formed. These results clearly show that the hydrophobic character of the catalyst is a necessary condition to obtain high activities and selectivities in epoxidation reactions with aqueous hydrogen peroxide solutions. Such a condition is achieved for TS-1, which explains its excellent performance in the epoxidation of linear olefins, but not for hydrophilic catalysts like Ti–Si mixed oxides or even Ti-β, for which the activity is very low.

REFERENCES

1. Sheldon, R. A., and Dakka, J., *Catal. Today* **19**(2), 215 (1994).
2. Miller, D. C., Sherrington, and Simpson, S., *J. Chem. Soc. Trans.* **2**, 2091 (1994).
3. Gontier, S., and Tuel, A., *Appl. Catal. A: General* **143**, 125 (1996).
4. Zhang, W., Fröba, M., Wang, J., Tanev, P. T., Wong, J., and Pinnavaia, T. J., *J. Am. Chem. Soc.* **118**, 9164 (1996).
5. Corma, A., Navarro, M. T., and Perez-Pariente, J., *J. Chem. Soc. Chem. Commun.*, 147 (1994).
6. Imamura, S., Nakai, T., Kanai, H., and Ito, T., *J. Chem. Soc. Faraday Trans.* **91**(8), 1261 (1995).
7. Liu, Z., Crumbaugh, G. M., and Davis, R. J., *J. Catal.* **159**, 83 (1996).
8. Imamura, S., Nakai, T., Kanai, H., and Ito, T., *Catal. Lett.* **28**, 277 (1994).
9. Hutter, R., Dutoit, D. C. M., Mallat, T., Schneider, M., and Baiker, A., *J. Chem. Soc. Chem. Commun.*, 163 (1995).
10. Klein, S., Thorimbert, S., and Maier, W. F., *J. Catal.* **163**, 476 (1996).
11. Dutoit, D. C. M., Schneider, M., and Baiker, A., *J. Catal.* **153**, 177 (1995).
12. Dutoit, D. C. M., Schneider, M., and Baiker, A., *J. Catal.* **153**, 165 (1995).
13. U.S. Patent 1,249,079 (1971), to Shell Oil.
14. Wulff, U.S. Patent 3,923,843 (1975) to Shell Oil.
15. Ellestad, O. H., and Blindheim, U. J., *Mol. Catal.* **33**, 275 (1985).
16. Kooyman, P. J., Van der Waal, P., Verdaasdonk, P. A. J., Jansen, K. C., and Van Bekkum, H., *Catal. Lett.* **13**, 229 (1992).
17. Haukka, S., Lakomaa, E. L., Jylha, O., Vilhunen, J., and Hornytzkyj, S., *Langmuir* **9**, 3497 (1993).
18. Kinney, J. B., and Staley, R. H., *J. Phys. Chem.* **87**, 3735 (1983).
19. Riis, T., Dahl, I. M., and Ellestad, O. H., *J. Mol. Catal.* **18**, 203 (1983).
20. Haukka, S., Lakomaa, E. L., and Root, A., *J. Phys. Chem.* **97**, 5085 (1993).
21. Fraile, J. M., Garcia, J. I., Mayoral, J. A., De Menorval, L. C., and Rachdi, F., *J. Chem. Soc. Chem. Commun.*, 539 (1995).
22. Srinivasan, S., Datye, A. K., Smith, M. H., and Peden, C. H. F., *J. Catal.* **145**, 565 (1994).
23. Olroyd, R. D., Thomas, J. M., Maschmeyer, T., MacFaul, P. A., Snelgrove, D. W., Ingold, K. U., and Wayner, D. D. M., *Angew. Chem. Int. Ed. Engl.* **35**(23/24), 2787 (1996).
24. Neumann, R., Chava, M., and Levin, M., *J. Chem. Soc. Chem. Commun.*, 1685 (1993).
25. Khouw, C. B., Dartt, C. B., Labinger, J. A., and Davis, M. E., *J. Catal.* **149**, 195 (1994).
26. Sheldon, R. A., *J. Mol. Catal.* **7**, 107 (1980).
27. Jorda, E., Tuel, A., Teissier, R., and Kervennal, J., *J. Chem. Soc. Chem. Commun.*, 1175 (1995).
28. Jorda, E., Teissier, R., Tuel, A., and Kervennal, J., Eur. Pat. Appl. 08/773,042 (1997).
29. Liu, Z., and Davis, R. I., *J. Phys. Chem.* **98**, 1253 (1994).
30. Klein, S., Weckhuysen, B. M., Martens, J. A., Maier, W. F., and Jacobs, P. A., *J. Catal.* **163**, 489 (1996).
31. Lang, S. J., and Morrow, B. A., *J. Phys. Chem.* **98**, 13314 (1994).
32. Trong On, D., Bonneviot, L., Bittar, A., Sayari, A., and Kaliaguine, S., *J. Mol. Catal.* **74**, 233 (1992).
33. Ko, E. I., Chen, J. P., and Weissman, J. G., *J. Catal.* **105**, 511 (1987).
34. Doolin, P. K., Alerasool, S., Zalewski, D. J., and Hooffman, J. F., *Catal. Lett.* **25**, 209 (1994).
35. Galan-Fereres, M., Alemany, L. J., Mariscal, R., Banares, M. A., Anderson, J. A., and Fierro, L. G., *Chem. Mater.* **7**, 1342 (1995).
36. Kataoka, T., and Dumesic, J. A., *J. Catal.* **112**, 66 (1988).
37. Miller, J. B., and Ko, E. I., *J. Catal.* **159**, 58 (1996).
38. Muscas, M., Solinas, V., Gontier, S., Tuel, A., and Auroux, A., *Stud. Surf. Sci. Catal.* **94**, 101 (1995).
39. Fusi, A., Ugo, R., and Zanderighi, G. M., *J. Catal.* **34**, 175 (1994).
40. Lempers, H. E. B., Chen, J. D., and Sheldon, R. A., *Stud. Surf. Sci. Catal.* **94**, 705 (1995).